

Electronic Supplementary Material (ESI) for Nanoscale.
This journal is © The Royal Society of Chemistry 2023

Supporting Information

Bacterially Synthesized Superfine Tellurium Nanoneedles as An Antibacterial and Solar-Thermal Still for Efficient Clean Water Purification

*Yu Wang, Zhongming Huang, Yijian Gao, Jie Yu, Jie Zhang, Xiliang Li, Yuliang Yang,
Qi Zhao, and Shengliang Li**

Dr. Y. Wang, Dr. Z. Huang, Y. Gao, J. Yu, J. Zhang, X. Li, Y. Yang, Dr. Q. Zhao,

Prof. S. Li

College of Pharmaceutical Sciences, Soochow University, Suzhou, 215123, P. R.
China

E-mail: lishengliang@suda.edu.cn

Materials

S. oneidensis MR-1 (ATCC 700550) was purchased from China Center for Type Culture Collection (CCTCC). Gram-positive *S. aureus* and gram-negative *E. coli* 25922 were obtained from the Guangdong Microbial Culture Collection Center. Sodium tellurite (Na_2TeO_3) was purchased from Sigma-Aldrich Hong Kong Holding Limited, (Hong Kong, China). Casein tryptone and peptone were purchased from Aladdin (Shanghai, China). Luria-Bertani (LB) medium, agar powder and NaCl were provided by Sinopharm Chemical Reagent Co., Ltd. (Shanghai, China). Hexadecyl trimethyl ammonium bromide (CTAB) and polyvinyl alcohol (PVA) were purchased from Sigma-Aldrich Co., Ltd. (Shanghai, China). The filtered natural seawater was obtained from Huiquan bay, Qingdao, China. Methylene blue (MB) and ionic standard solutions including Na^+ (100 $\mu\text{g}/\text{mL}$), K^+ (100 $\mu\text{g}/\text{mL}$), Mg^{2+} (100 $\mu\text{g}/\text{mL}$), Ca^{2+} (100 $\mu\text{g}/\text{mL}$), Fe^{3+} (1000 $\mu\text{g}/\text{mL}$), Co^{2+} (100 $\mu\text{g}/\text{mL}$), Ni^{2+} (500 $\mu\text{g}/\text{mL}$), Cu^{2+} (1000 $\mu\text{g}/\text{mL}$), Ag^+ (100 $\mu\text{g}/\text{mL}$), Hg^{2+} (100 $\mu\text{g}/\text{mL}$), Pb^{2+} (100 $\mu\text{g}/\text{mL}$), Cd^{2+} (1000 $\mu\text{g}/\text{mL}$) were purchased from Aladdin (Shanghai, China).

Measurements

Absorption spectra were recorded by UV-VIS-NIR spectrophotometer (PE950, Perkin Elmer, USA). Transmission electron microscopy (TEM) images were carried out using a transmission electron microscope (TALOS 200X, Thermo Scientific, USA). Size and zeta potential were taken on a Nano ZS90 (Malvern, UK) instrument. Scanning electron microscopy (SEM) images were carried out using a scanning electron microscope (SU8230, Hitachi, Japan), and the corresponding elemental spectra were detected by

energy dispersive spectrometer (EDS, Aztec X-MAX80, OXFORD, UK). A solar simulator (HM-Xe500W) equipped with an optical filter for the standard AM 1.5 G spectrum were purchased from Changchun New Industries Optoelectronics Tech. Co., Ltd (Changchun, China). The temperature variations were recorded with a thermal imaging camera (Fluke Ti400, IR Fusion Technology, USA). The wettability was measured using a contact angle measuring device (Dataphysics OCA15EC, Germany). The content of ions in solution was detected by inductively coupled plasma optical emission spectroscopy (ICP-OES, Avio200, Germany).

Bacteria Culture

The *S. oneidensis* MR-1 was cultured in Casein Soya Bean Digest Agar (TSA) medium (15 g/L casein tryptone, 5 g/L peptone and 5 g/L NaCl). A single colony was picked and inoculated into 30 mL of TSA medium, putting it in a swing bed (SHZ- 82 A, HUARUIKEQI) with 180 rpm/min at 30 °C overnight. And coating plate method based on the protocol of ASTM D5465-16 was used to estimate the number of active *S. oneidensis* MR-1 in culture medium at different time to obtain the growth curve.

Biosynthesis of Te@SOM

According to the growth curve, *S. oneidensis* MR-1 in stable phase was collected in 50 mL sterile centrifuge tubes and centrifuged at 6000 rpm for 5 min, washing three times using PBS solution. The as-obtained *S. oneidensis* MR-1 cells were resuspended in 20 mL PBS including Na₂TeO₃ with various concentrations, incubating in a shaking incubator (30 °C, 180 rpm) for a certain period of time.^{1,2} After that, the solution was centrifuged and washed with ultrapure water three times to remove the excess PBS

before handling by ultrasonication for 20 min with a power of 200 W. And then the solution was centrifuged at 5000 rpm for 10 min and filtrated with 0.45 and 0.22 μm to remove large particles respectively. Finally centrifuging at 14000 rpm to concentrate it. Thus, we obtained the biosynthetic Te NDs covered by bacterial debris, named Te@SOM. Furthermore, the single Te NDs was separated from bacterial debris via ultrasonication with CTAB.

Characterization of Te@SOM

TEM images of bacterial cell containing Te NDs and assisted element mapping were carried out using a TALOS 200X at the acceleration voltage of 200 kV. The absorption spectra of Te@SOM and single Te NDs solutions were detected by PE950. Dynamic light scattering (DLS) and zeta potential of various dispersion liquids were measured by Zetasizer Nano ZS90. For quantitative test, the content of Te in Te@SOM was measured by ICP-OES after digestion.

Fabrication procedure of TSAS scaffold

PVA (1 g), glutaraldehyde (125 μL , 50%wt) and ultrapure water (10 mL) were mixed together, stirring overnight to ensure thorough dissolution. And then Te@SOM solutions were added into PVA solution with a volume ratio of 2:3 to obtain various final concentrations of Te@SOM. Meanwhile, HCl (50 μL , 1.2M) solution was mixed into it. The gelation was carried out for 2 h. The as-obtained PVA gel was immersed into DI water overnight. And then the PVA gel was frozen by $-80\text{ }^{\circ}\text{C}$ refrigerator and thawed in DI water with a temperature of $30\text{ }^{\circ}\text{C}$, repeating for 5 times.³ Finally, the PVA gel samples loaded with different amounts of Te@SOM was freeze-dried

overnight to obtain a series of TSAS scaffolds, they were TSAS-1 (50 $\mu\text{g}/\text{mL}$), TSAS-2 (100 $\mu\text{g}/\text{mL}$); TSAS-3 (150 $\mu\text{g}/\text{mL}$); TSAS-4 (200 $\mu\text{g}/\text{mL}$); TSAS-5 (300 $\mu\text{g}/\text{mL}$), respectively. Absorption spectra of pristine PVA scaffold and TSAS-3 were conducted by UV-VIS-NIR spectrophotometer. The microstructures and elemental mapping were obtained by SEM and EDS. The wettability of pristine PVA scaffold and TSAS-3 was evaluated by a contact angle measuring device.

Photothermal performance of TSAS scaffold

The photothermal performances of TSAS under a solar simulator (HM-Xe500W) equipped with an optical filter for the standard AM 1.5 G spectrum were tested, including the samples with and without immersion in water. And the photothermal stability of TSAS was evaluated by 5 on/off cycles upon 1 Sun light irradiation. Meanwhile, the temperature was monitored by infrared imaging devices (FLUKE) at regular intervals.

Solar water evaporation

Solar water evaporation experiments were performed using the solar simulator at an ambient of 25 $^{\circ}\text{C}$ and humidity 45%. The TSAS-3 with a size of 10 mm diameter and 10 mm thickness was freely floated on a beaker filled with water. Mass of water evaporated was measured every 5 min with a high accuracy balance during one hour evaporation under 1 Sun illumination, and the evaporation rates of utilized scaffolds were calculated. The solar energy conversion efficiency (η) is another important parameter in solar steam generation, which can be calculated via the following equation:⁴

$$\eta = \frac{mh_v}{C_{opt}P_o} \quad (1)$$

where m is the net evaporation rate calculated by subtracting the evaporation rates under the dark condition from the measured evaporation rates. h_v is the water evaporation enthalpy, P_o is the solar irradiation power of 1 sun (1.0 kW m^{-2}), and C_{opt} is the optical concentration.

Seawater desalination and water purification of sewage

The performance of seawater desalination using TSAS-3 was evaluated via comparing the contents of Na^+ , K^+ , Mg^{2+} , Ca^{2+} in seawater before and after evaporation. The form floated on surface of seawater under 1 Sun illumination. And then steam attached to the glass wall that was generated. The sewages including MB, heavy metal (Fe^{3+} , Co^{2+} , Ni^{2+} , Cu^{2+} , Hg^{2+} , Ag^+ , Pb^{2+} , Cd^{2+}) and bacteria (*E. coli* and *S. aureus* solutions) were treated similarly. The absorption spectra of MB solution before and after evaporation were used to evaluate the purification performance of organic solvent. And the content of main ions in heavy metal sewages were detected by ICP-OES. The antibacterial rate was tested by plate method.⁵ Furthermore, the antibacterial ability of the form was assessed by zone of inhibition (ZOI) of *E. coli* and *S. aureus*.



Figure S1. Digital photographs of *S. oneidensis* MR-1 solutions without/ with TeO₃²⁻ after 6 h coculture.

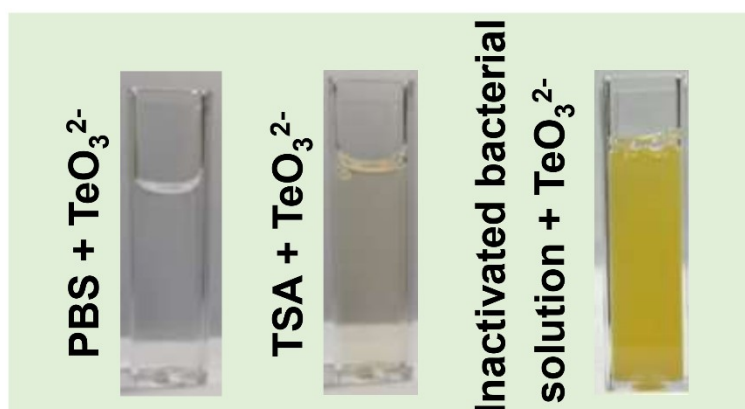


Figure S2. Digital photographs of various solutions cocultured with TeO₃²⁻ for 6 h.

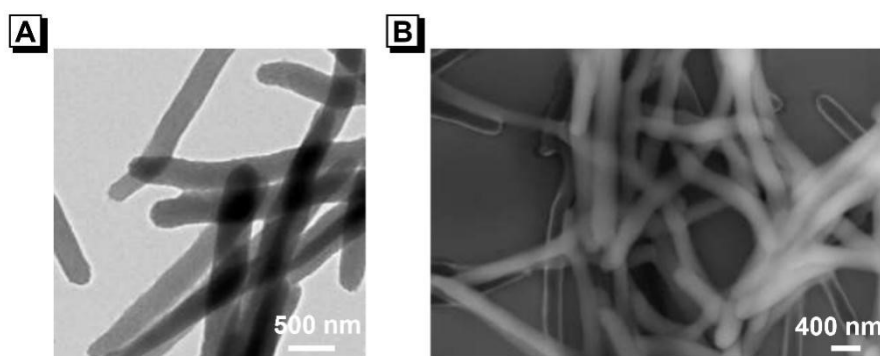


Figure S3. TEM (A) and SEM (B) images of *S. oneidensis* MR-1 without TeO₃²⁻.

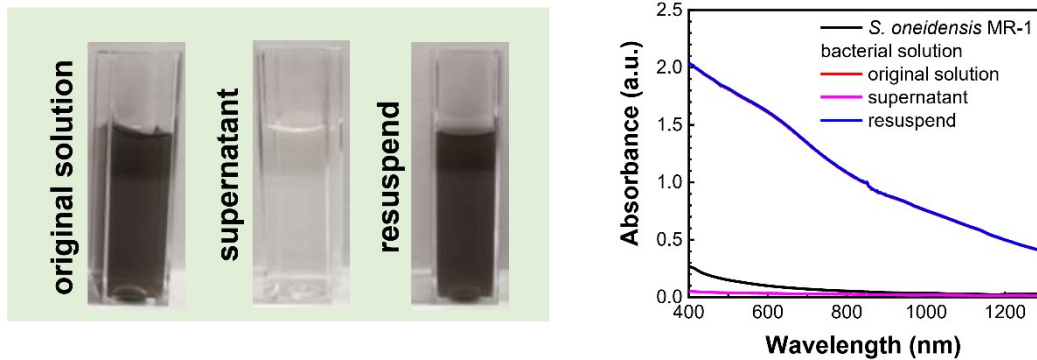


Figure S4. Macroscopic images and the corresponding UV-Vis curves of *S. oneidensis* MR-1 co-cultured with TeO_3^{2-} after different treatment.

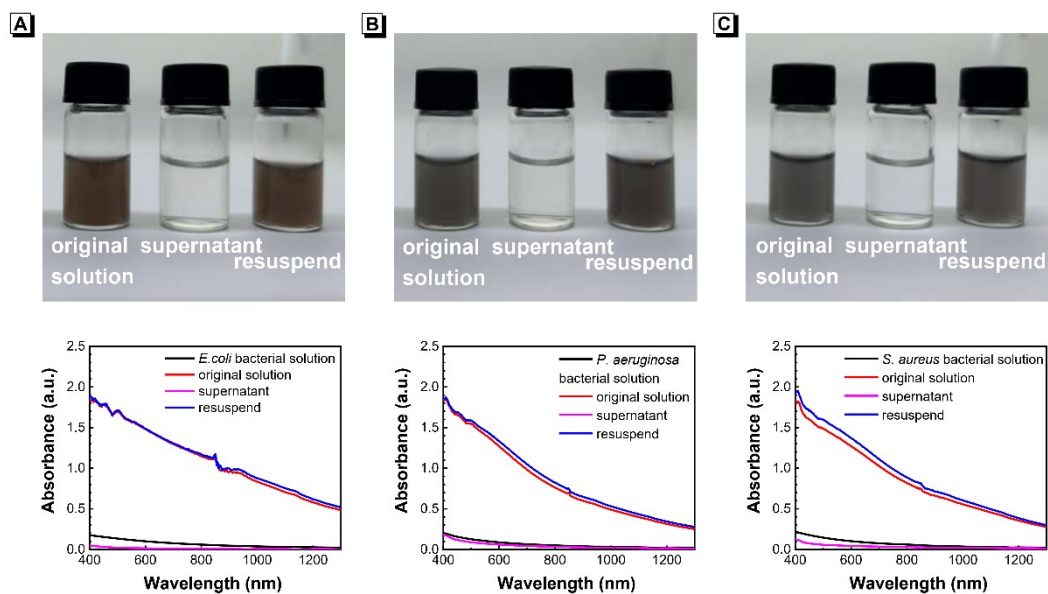


Figure S5. Macroscopic images and the corresponding absorption curves of *E. coli* (A), *P. aeruginosa* (B), and *S. aureus* (C) co-cultured with TeO_3^{2-} after different treatments.

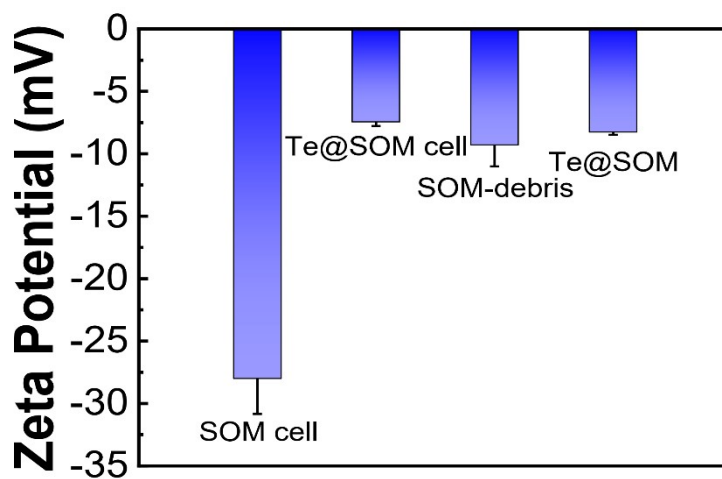


Figure S6. The zeta potential of various *S. oneidensis* MR-1 dispersion solutions.

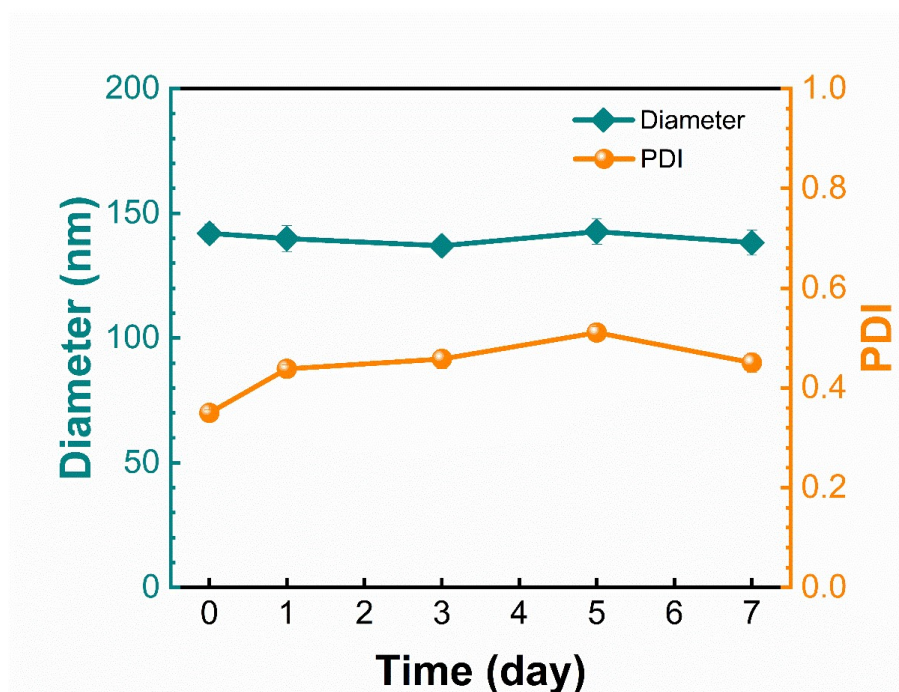


Figure S7. Stability analysis in size and PDI of Te@SOM aqueous solution within 7-day storage.



Figure S8. Digital photographs of pristine PVA scaffold and TSAS-1 ~ TSAS-5.

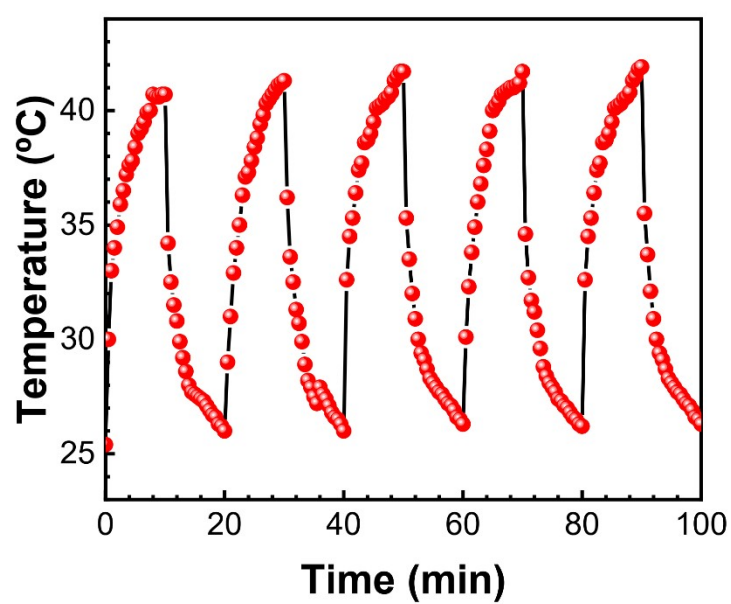


Figure S9. Photothermal stability of TSAS-3 upon 1 Sun light irradiation for five on/off cycles.

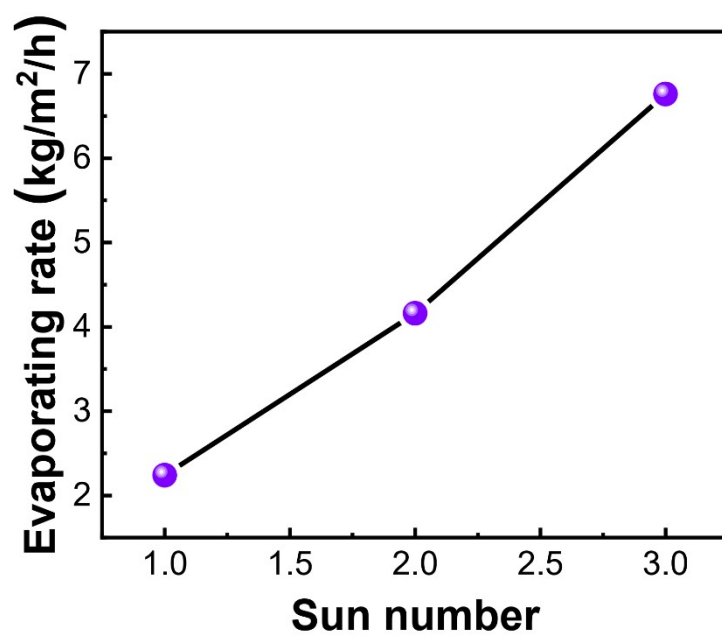


Figure S10. Evaporation rates of TSAS-3 upon 2 Sun and 3 Sun light illumination.



Figure S11. Digital photo of TSAS-3 after 14 days immersion.

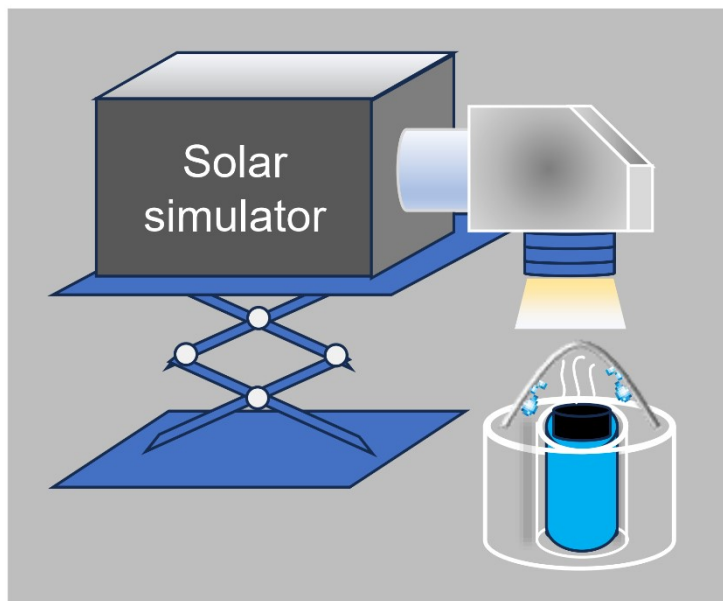


Figure S12. Schematic illustration of a water-collecting system for solar water purification.

References:

- [1] D.H. Kim, M.G. Kim, S. Jiang, J.H. Lee, H.G. Hur, *Environ. Sci. Technol.* **2013**, 47, 8709-8715.
- [2] Y. Yao, J. Li, P. Li, D. Wang, W. Bao, Y. Xiao, X. Chen, S. He, J. Hu, X. Yang, *Small* **2022**, 18, 2105716.
- [3] F. Zhao, X. Zhou, Y. Shi, X. Qian, M. Alexander, X. Zhao, S. Mendez, R. Yang, L. Qu, G. Yu, *Nat. Nanotechnol.* **2018**, 13, 489-495.
- [4] X. Zhou, Y. Guo, F. Zhao, W. Shi, G. Yu, *Adv. Mater.* **2020**, 32, 2007012.
- [5] Y. Yang, L. Yang, F. Yang, W. Bai, X. Zhang, H. Li, G. Duan, Y. Xu, Y. Li, *Mater. Horiz.* **2023**, 10, 268-276.